

# Petri net based cluster and reachability analysis of the heat shock response in eukaryotes

Tseren-Onolt Ishdorj  
Department of Computer Science,  
School of Information and  
Communication Technologies  
Mongolian University of  
Science and Technology  
eMail: tseren-onolt@must.edu.mn

Baatarkhuu Enkhtuya  
Department of Info Technology  
School of Information and  
Communication Technologies  
Mongolian University of  
Science and Technology  
eMail: baatarkhuu@must.edu.mn

Choisuren Ragchaabazar  
Department of Mathematics  
School of Applied Sciences  
Mongolian University of  
Science and Technology  
eMail: rchoi@must.edu.mn

**Abstract**—From computer modelling point of view, biological system itself highly parallel, distributed, and concurrent mechanism in its functioning. On the otherhand, a software engineering formal method Petri net is widely used in modelling for distributed and concurrent systems. We consider a qualitative model based on Petri nets for the eukaryotic heat shock response introduced in [1]. The heat shock response (HSR) is a very well conserved defense mechanism against protein misfolding. The network includes mechanisms for *feed-forward amplification, feed-back regulation and stress-induced activation*. In the present paper based on a recently introduced clustering approach for biochemical Petri nets, we explore and identify the main functional, biologically-relevant modules of the heat shock response model. We also explore its reachability properties and interpret them in terms of viability of the heat shock response.

## I. INTRODUCTION

### A. The heat shock response

The heat shock response is the reaction of cells to elevated temperatures. Under raised temperature (or other stress stimuli such as heavy metals or radiation), proteins tend to misfold and then form big aggregates that may eventually render the cell unable to survive, see [2]. It is well understood that the main role in the cell's reaction to heat shock is played by the heat shock proteins (HSP), see [3], [4]. They act as chaperons, helping misfolded proteins (MFP) to refold into their native form (PROT). The heat shock proteins have a major contribution also in the resilience of cancer cells, see [5] and they have been suggested as targets in potential cancer treatments, see [6], [7].

In eukaryotes, the heat shock response is controlled through the regulation of the transactivation of the HSP-encoding genes, see [4], [8] (the bacterial mechanisms is

only slightly different, see [9]). The kinetic details of the control have been disputed in the past few years, with several models proposed in [8], [10], [11]. We follow in this paper a molecular model of a new kinetic model for the heat shock response proposed in [12]. In this model, the transcription of the gene is promoted by some proteins called heat shock factors (HSF) that dimerize (HSF2) and then trimerize (HSF3), eventually bind to a specific DNA sequence called heat shock element (HSE), upstream of the HSP-encoding gene. Once the HSF3 is bound to the HSE, the gene is transactivated and the synthesis of HSP is thus switched on. Once the level of HSP is high enough, the cell has an ingenious mechanism to switch off its own synthesis. For this, HSPs bind to free HSFs, as well as breaking the HSF trimers (including those bound to HSEs, promoting the gene activation), thus effectively halting the HSP synthesis. In this model we treat uniformly under HSP all types of heat shock proteins. We have a similar convention for treating uniformly all three types of heat shock factors under the name HSF. PROT and MFP group together all proteins and misfolded proteins, respectively, other than HSP and HSF. Table I summarizes the list of reactions used in [13] from the the kinetic model of [12]. In the table we list each reversible reaction as two irreversible ones, accounting for its two directions.

### B. Petri nets and clustering

Let us give here the basic notions and notations of a Petri net which are used through the paper, for the detailed introduction the reader is referred to, for instance, [14], [15].

A *Petri net* consists of *places*, represented as circles; *transitions*, represented as boxes; *arrows from places to transitions*; arrows from transitions to places; a *weight*

for every arrow (represented as a number), weight '1' can be omitted; a *marking* is indicated by the number of tokens in every place; an *initial marking*, defining the initial number of tokens for every place.

In a Petri net, a place  $p$  is in the *pre-set* (or *post-set*) of a transition  $t$  if there is an arrow from  $p$  to  $t$  (or an arrow from  $t$  to  $p$ ); a transition  $t$  is *enabled* if for every place  $p$  from the pre-set of  $t$  the weight of the arrow from  $p$  to  $t$  is not greater than the number of tokens indicated at  $p$ . An enabled transition  $t$  will *occur* in that the number of tokens at every place  $p$  is decreased by  $g$  if the arrows from  $p$  to  $t$  are of weight  $g$  and in that the number of tokens at every place  $p'$  is increased by  $g'$  if the arrows from  $t$  to  $p'$  are of weight  $g'$ . Two transitions are in conflict with one another if both are enabled and the occurrence of one results in the disablement of the other, but one of them occur chosen non-deterministically. A transition is *deadlocked* if it can never fire. A transition is *live* if it can never deadlock.

Consider a Petri net  $\mathcal{P}$  with the set of places  $P = \{p_1, \dots, p_n\}$  and set of transitions  $T = \{t_1, \dots, t_m\}$ , for some  $m, n \geq 1$ . Its *incidence matrix*  $A$  is an  $(n \times m)$ -matrix (where  $n$  denotes the number of places and  $m$  the number of transitions). Every matrix entry  $a_{ij}$  gives the token change on the place  $p_i$  by the firing of the transition  $t_j$ . Thus, firing transition  $t_j$  changes the state of the system from  $M \in \mathbb{N}_0^n$  to state  $A_j + M$ , where  $A_j$  is the  $j$ -th column of  $A$ . The transition may fire if and only if all entries of  $A_j + M$  are nonnegative integers.

A *T-invariant* is defined as a non-zero vector  $x \in \mathbb{N}_0^m$ , which holds the equation  $A \cdot x = 0$ . A T-invariant represents a multiset of transitions, which have altogether a zero effect on the marking. Analogously, a *P-invariant* is defined as a non-zero vector  $y \in \mathbb{N}_0^n$  such that  $y^t \cdot A = 0$ , where  $y^t$  is the row-vector transpose of  $y$ . A P-invariant characterizes a token conservation rule for a set of places, over which the weighted sum of tokens is constant independently from any firing.

The *reachability set*  $R(M)$  of a net is the set of all markings  $M$  reachable from initial marking  $M_0$ . A Petri net is called *bounded* if and only if the initial marking  $M_0$  is finite and there exists  $k \in \mathbb{N}$  such that, for all marking  $M$  reachable from the initial marking and all places  $p \in P$ ,  $M(p) \leq k$  i.e. places never hold more than  $k$  tokens.

Cluster analysis comprises a range of methods for classifying multivariate data into subsets (clusters) based on similarity. Clustering is the process of organizing objects into groups whose members are similar to one

another. Thus, a cluster is a collection of similar objects. By partitioning heterogeneous data into relatively homogeneous clusters, clustering can help to identify the intrinsic grouping in the data set and to reveal the characteristics of some structure in the data. A cluster analysis can be seen as a three step process, encompassing the following main steps: (1) selection of a distance measure to compute the distance between all pairs of objects, (2) selection of a clustering algorithm to group the objects based on the computed distances, and (3) selection of a cluster validity measure to identify the optimal number of clusters for interpretation.

We follow in this paper a cluster analysis approach for Petri nets proposed in [16] with the aim of decomposing biochemical networks into functional modules. In this approach, the T-invariants of the Petri net are clustered. This in turn induces a clustering of the model, where different clusters may have nodes and transitions.

The *Tanimoto* distance measure [17] among other measuring methods can be used to classify T-invariants, [16]. The *Tanimoto* coefficient, measuring the similarity between two T-invariants,  $t_i$  and  $t_j$ , is computed as follows:

$$s(t_i, t_j) = s_{ij} = \frac{a}{(a + b + c)}$$

where  $a$  is the number of transitions common in both  $t_i$  and  $t_j$ ,  $b$  is the number of transitions only present in  $t_i$ , and  $c$  is the number of transitions only present in  $t_j$ . The *Tanimoto* coefficient is then transformed into a distance,  $d_{ij}$ , by

$$d_{ij} = 1 - s_{ij}.$$

Having obtained the distance between each pair of objects, a number of clustering algorithms such as *UPGMA* (*Unweighted Pair Group Method with Arithmetic mean*), *Complete Linkage*, *Single Linkage* and *PAM* (*Partition Around Medoids*) can be applied. For instance, in an agglomerative clustering algorithm *UPGMA*, which is used in this paper, the distance between two clusters,  $C_i$  and  $C_j$ , is computed as the average of distances,  $d_{ij}$ , of all possible pairs of objects with  $i \in C_i$  and  $j \in C_j$ . Whereas the clustering starts with the finest partitioning (singleton), merging the two most similar clusters in each iteration, until all clusters are joined in one cluster.

To select the optimal number of clusters, one may use the *Silhouette Width* [18] as a cluster validity measure. For each object  $i$  in cluster  $A_i$ , the *Silhouette value*  $s_i$  is calculated as follows:

$$s_i = \frac{b_i - a_i}{\max(a_i, b_i)}$$

where  $a_i$  is the average distance of object  $i$  to all objects of the cluster  $A_i$  and  $b_i$  is the average distance of object  $i$  to all objects of the closest cluster  $B_i$  (neighbor of object  $i$ ). Intuitively, the Silhouette value is giving a measure for whether object  $i$  was placed in the most suitable cluster:

- values near 1 indicate that an object is near the center of a tight cluster;
- values near 0 indicate that an object is between clusters;
- negative values indicate that an object may be in the wrong cluster.

Average Silhouette width is the average of  $s_i$  for all objects  $i$  in the data, i.e. average Silhouette width for  $k$  clusters. This can be used to select the "best" number of clusters, by choosing that  $k$  yielding the highest average of  $s_i$ . One may then select the number of clusters in such a way that the average Silhouette width over all T-invariants is maximized. We denote by SC (Silhouette coefficient) the average Silhouette width of the resulting clustering.

The SC coefficient can then be used to decide on the quality of the resulting clustering (see [19]):

- if SC is between 0.71 and 1.00, then a strong structure has been found;
- if SC is between 0.51 and 0.70, then a reasonable structure has been found;
- if SC is between 0.26 and 0.50, then the structure is weak and could be artificial, please try additional methods on this data;
- if SC is less than 0.25, then no substantial structure has been found.

## II. MODELING METHOD

Each species in the molecular model is represented as a place in the Petri net, labeled by  $p_1, p_2, \dots, p_{10}$ , while the reactions in the model are represented as transitions injectively labeled by  $t_0, t_1, \dots, t_{16}$  as indicated in Table I.

We illustrate in Figure 1 each type of (1) – (8) reactions as Petri net components, whereas the species involved in a reaction are represented by pre-places, the reaction itself represented by a transition, while the reaction results or produced species are the post-places, thus, a chemical reaction is represented as a transition occurrence of Petri net.

When composing the Petri net components corresponding to all reactions (by merging the places with identical labels of species), we obtain the Petri net model  $\mathcal{P}$  of the heat shock response consists of 10 places and 17 transitions, described in [1].

The tokens in a place represents the number of copies of the corresponding species existing in the model at the time. The incidence matrix of the Petri net model  $\mathcal{P}$  is described in [1].

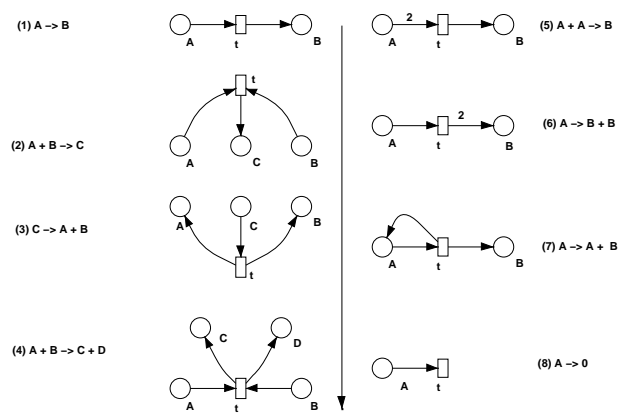


Fig. 1. 8 basic type of Petri net components for HSR model.

We consult the reader refer to [1] where one can find various results based on P-Invariant and T-Invariant analysis of the Petri net model of heat shock response.

a) *Clustering the network*: Consider now the clustering of the net and see how the net structure is composed of distinct modules relevant to biological meaningful functions.

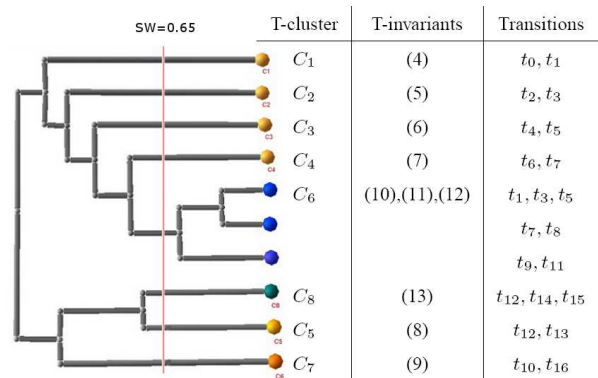


Fig. 2. The dendrogram for the T-clusters and corresponding T-invariants composed of transitions.

In our T-cluster analysis, the *Tanimoto* coefficient, see Section I-B, is used to measure the similarity between T-invariants, which is implemented by the PInA [20]. Having obtained the distance matrix, a hierarchical (*UP-GMA*) and a partitioning (*PAM*) clustering algorithms are applied. Finally, to determine the optimal number of T-clusters for interpretation, the *Silhouette Width*,

TABLE I

THE METABOLITES AND REACTIONS IN THE MOLECULAR MODEL OF THE HEAT SHOCK RESPONSE OF [12]. THEY ARE MODELED AS PLACES AND TRANSITIONS, RESPECTIVELY, IN PETRI NET APPROACH IN [1].

Places	Metabolite	Transition	Reaction
$p_1$ :	$HSE$	[HSF3 unbd HSE] $t_0$ :	$HSF3 : HSE \rightarrow HSF3 + HSE$
$p_2$ :	$HSF3 : HSE$	[DNA bnd] $t_1$ :	$HSF3 + HSE \rightarrow HSF3 : HSE$
$p_3$ :	$HSF3$	[detrimer] $t_2$ :	$HSF3 \rightarrow HSF2 + HSF$
$p_4$ :	$HSF2$	[trimer] $t_3$ :	$HSF2 + HSF \rightarrow HSF3$
$p_5$ :	$HSF$	[monomer] $t_4$ :	$HSF2 \rightarrow 2HSF$
$p_6$ :	$HSP : HSF$	[dimer] $t_5$ :	$2HSF \rightarrow HSF2$
$p_7$ :	$HSP$	[HSP bnd HSE] $t_6$ :	$HSP + HSF \rightarrow HSP : HSF$
$p_8$ :	$MFP$	[HSF3 unbd HSE] $t_7$ :	$HSP : HSF \rightarrow HSP + HSF$
$p_9$ :	$PROT$	[brk trimer] $t_8$ :	$HSP + HSF3 \rightarrow HSP : HSF + 2HSF$
$p_{10}$ :	$HSP : MFP$	[brk dimer] $t_9$ :	$HSP + HSF2 \rightarrow HSP : HSF + HSF$
		[HSP prod] $t_{10}$ :	$HSF3 : HSE \rightarrow HSF3 : HSE + HSP$
		[DNA unbd] $t_{11}$ :	$HSP + HSF3 : HSE \rightarrow HSP : HSF + 2HSF + HSE$
		[chap.act] $t_{12}$ :	$HSP + MFP \rightarrow HSP : MFP$
		[chap.inact] $t_{13}$ :	$HSP : MFP \rightarrow HSP + MFP$
		[refold] $t_{14}$ :	$HSP : MFP \rightarrow HSP + PROT$
		[misfold] $t_{15}$ :	$PROT \rightarrow MFP$
		[HSP degrad] $t_{16}$ :	$HSP \rightarrow 0$

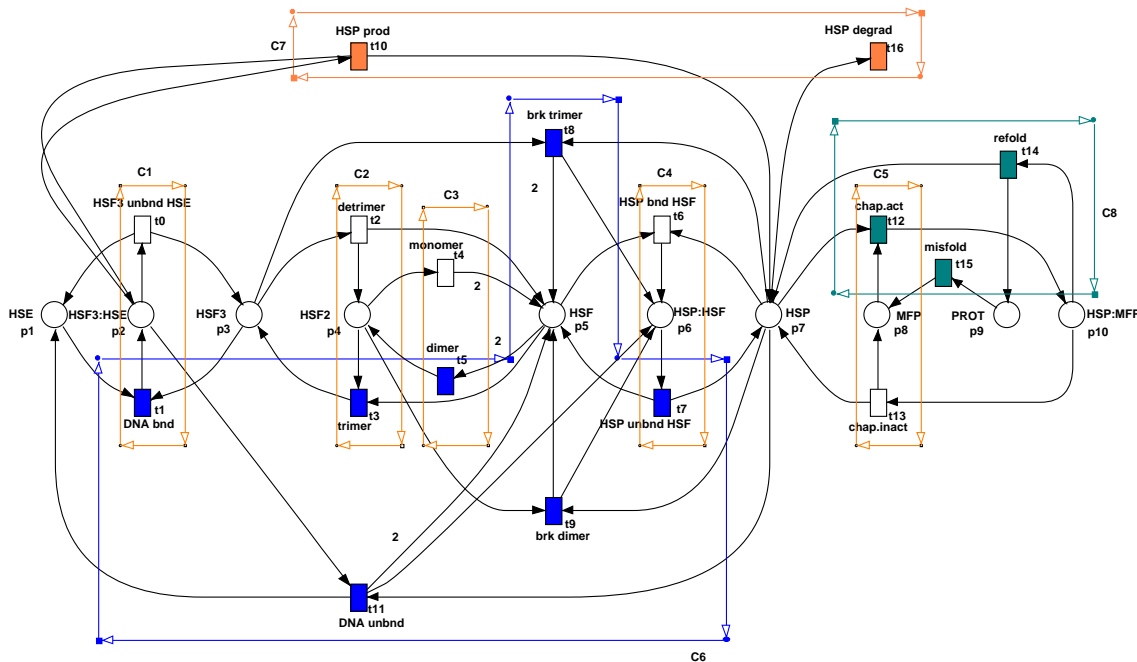


Fig. 3. The result of clustering the T-invariants of Petri net in Figure 2. The clusters are outlined.

see Section I-B, is checked among the cluster validity measures performed using *PInA* [20] and *WinIDAMS* [19]. The hierarchical clustering algorithms suggest to split the net into 8 T-clusters, while the partitioning clustering algorithm tells us 7 T-clusters could be the best among the others according to its cluster validity measure. As the result, we choice a clustering which partition the 10 T-invariants of the net into 8 distinct

T-clusters because it can sufficiently express biological meaningful modules of our biochemical Petri net. The dendrogram for the T-clustering, obtained by *PInA* [20] and visualized with *Wilmascope* [21], and the corresponding T-clusters composed of T-invariants within the transitions are illustrated in Figure 2 and also the obtained T-clusters are highlighted on our Petri net in Figure 3.

The T-invariants (4)–(8), presented in [1], are trivial: they form the T-clusters  $C_1, C_2, C_3, C_4$ , and  $C_5$ , which altogether represent the feed-forward amplification (gene transcription) mechanism. The non-trivial T-invariants (9)–(13) form three other disjunctive T-clusters  $C_6, C_7$ , and  $C_8$ . A subsequent combination of the modules express a specific pathway of the network switch from the steady state ( $C_6$ ) at temperature 37C to the gene transcription ( $C_7$ ) as temperature raises to 42C and then misfolded protein repairing mechanism ( $C_8$ ) is switched on provided the HSP synthesis has been activated, finally the module  $C_6$  is returned as stress went away. The main function of T-cluster  $C_6$  is devoted to the feed-back regulation of the *HSP* transactivation and it is the dominant part of the model under physiological conditions (at temperature 37C). Reactions in this T-cluster include heat shock factor dimerization, trimerization, binding to *HSE*, and the *HSP*-backregulation of all forms of *HSF*. This cyclic reactions have to be switched to the T-cluster  $C_7$  in order to activate the *HSP*-encoding gene for future transactivation of the *HSP* synthesis as well as degradation mechanism as cell is under stress.

The stress-induced activation mechanism is represented in the next main T-cluster  $C_8$ , where the process of the misfolding of proteins and the chaperon activity of *HSP*, whose activity is greatly increased under raised temperature, see the biological interpretation of T-invariant (13) in [1].

Thus, each T-cluster of  $C_6, C_7$  and  $C_8$  represents a functionally different module, but their ordered sequential combination suggests a minimal pathway of switch between the cell conditions at temperature 37C and 42C, respectively.

*b) Reachability analysis:* Now we consider the reachability problem for our Petri net. As an example, let the initial marking be  $M'_0 = (HSE, 0, 0, 0, 3HSP, 0, 0, 0, PROT, 0)$ . In this case, all transitions are eventually enabled, while the network is not bounded. It can be seen that  $M'_0$  is a minimal initial marking with this property. In this case the reachability graph is infinite, while the coverability graph consists of 48 nodes. As another example, let the initial marking be  $M_0 = (HSE, 0, 0, 0, HSF, 0, HSP, MFP, PROT, 0)$ , which does not satisfy the P-invariants because of *HSP*. In this case the net is bounded. There are only 10 markings  $x$  that are reachable from  $M_0$ , see Table II and Figure 4. A schematic view of the paths (transitions) from the initial marking to the reachable markings and between the markings are depicted in Figure 4.

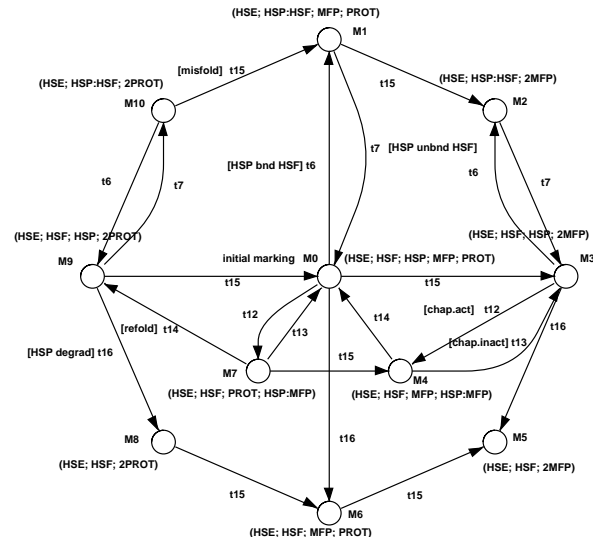


Fig. 4. Reachability graph from the marking  $M_0$ .

The following two results give some results about the reachability problem of our Petri net and about its possible deadlocks. The first result shows that a deadlock is characterized by the P-invariant given at (2) presented in [1].

**Proposition 1.** *The Petri net  $\mathcal{P}$  modeling the heat shock response may reach a deadlock starting from the initial marking  $M$  if and only if  $[p_2]3M(HSF3 : HSE) + [p_3]3M(HSF3) + [p_4]2M(HSF2) + [p_5]M(HSF) + [p_6]M(HSP : HSF) \leq 1$ . Equivalently,*

$p')$   $M(HSF3 : HSE) = M(HSF3) = M(HSF2) = 0$  and

$p'')$   $M(HSF) + M(HSP : HSF) \leq 1$ .

*Proof.* Assume first an initial marking  $M = (a, 0, 0, 0, n_1, n_2, b, c, d, e)$ , with  $a, b, c, d, e, n_1, n_2 \in \mathbb{N}$ ,  $n_1 + n_2 = 1$ . The following sequence of transitions leads to deadlock: ( $\rightarrow^{t^x}$  means a transition  $t$  applies  $x$  times in a row)

$$\begin{aligned} M &\rightarrow^{t_{15}^e} (a, 0, 0, 0, n_1, n_2, b, c, d + e, 0) \\ &\rightarrow^{t_{13}^c} (a, 0, 0, 0, n_1, n_2, b + c, 0, c + d + e, 0) \\ &\rightarrow^{t_7^{n_2}} (a, 0, 0, 0, 1, 0, b + c + n_2, 0, c + d + e, 0) \\ &\rightarrow^{t_{16}^{b+c+n_2}} (a, 0, 0, 0, 1, 0, 0, 0, c + d + e, 0). \end{aligned}$$

Assume now an initial marking  $M$  from where  $\mathcal{P}$  may reach a deadlock. Note that  $p = [p_2]3M(HSF3 : HSE) + [p_3]3M(HSF3) + [p_4]2M(HSF2) + [p_5]M(HSF) + [p_6]M(HSP : HSF)$  is a P-invariant of the Petri net and so, constant throughout the transitions of the Petri net. To conclude

TABLE II  
REACHABLE MARKINGS WITHIN THE INITIAL MARKING  $M_0 = (HSE, 0, 0, 0, HSF, 0, HSP, MFP, PROT, 0)$ .

	HSE	HSF3:HSE	HSF3	HSF2	HSF	HSP:HSF	HSP	MFP	PROT	HSP:MFP
$M_0$	1	0	0	0	1	0	1	1	1	0
$M_1$	1	0	0	0	0	1	0	1	1	0
$M_2$	1	0	0	0	0	1	0	2	0	0
$M_3$	1	0	0	0	1	0	1	2	0	0
$M_4$	1	0	0	0	1	0	0	1	0	1
$M_5$	1	0	0	0	1	1	0	2	0	0
$M_6$	1	0	0	0	1	0	0	1	1	0
$M_7$	1	0	0	0	1	0	0	1	1	1
$M_8$	1	0	0	0	1	0	0	0	2	0
$M_9$	1	0	0	0	1	0	1	0	2	0
$M_{10}$	1	0	0	0	0	1	0	0	2	0

the theorem, it is enough to show that if at least either condition  $p'$  or  $p''$  does not hold, then at least one transition is enabled to  $M$ . Assume then that  $p')$   $M(HSF3 : HSE) = M(HSF3) = M(HSF2) > 0$ . Then at least one token exists on either places. If  $M(HSF3 : HSE) \geq 1$ , then transition  $t_{10}$  is enabled infinitely, if  $M(HSF2) \geq 1$ , transitions  $t_4$  and  $t_5$  alter (trap) forever. Finally, if  $M(HSF3) \geq 1$ , then  $t_2, t_3, t_4, t_5$  are always enabled in some ways, in other words, a cycle of formations of  $HSF$  monomer, dimer, trimer is enabled indefinitely. On the other hand, assume  $p'')$   $M(HSF) + M(HSP : HSF) > 1$ . Let us check a case of two tokens existence such that  $M(HSF) + M(HSP : HSF) = 2$ . There are three possibilities: 1) if  $M(HSF) = 2$ , then forever alternating of transitions  $t_5$  and  $t_4$  is enabled; 2) if  $M(HSP : HSF) = 2$ , by occurrences of transition  $t_7$ , the case 1) is always obtained; 3) in a case  $M(HSF) = M(HSP : HSF) = 1$ , again case 1) is always reachable. Thus, a deadlock is possible if and only if the conditions  $p'$  and  $p''$  are held.  $\square$

Our second result relates the reachability problem to the P-invariants (1) – (2) in [1].

### III. CONCLUSION

The invariants of the Petri net model correspond to properties of the continuous model of [12]: the P-invariants correspond to the mass-conservation relations and the T-invariants correspond to the elementary modes. This relation follows from the fact that the incidence matrix of the Petri net model coincides with the stoichiometric matrix of the continuous model and has been reported

many times before, see, e.g., [22]. The types of analysis one can perform with the two approaches are however completely different. While the continuous model gives interesting steady state analysis, including sensitivity analysis, the Petri net allows reasoning about the network itself, albeit in qualitative, rather than quantitative terms. The Petri net of the heat shock response satisfies the model validation criteria according to [23], [24]: the net is covered by minimal T-invariants; each T-invariant and the clusters built by T-invariants can be interpreted as biologically meaningful distinct functions/modules. We gave in Theorem 1 a simple condition for the network to run indefinitely, regardless of the transitions to be fired along any path.

Moreover, we studied the network from cluster analysis point of view and discovered biologically meaningful functions for the signalling pathway. For instance, the T-clusters  $C_1, C_2, C_3, C_4$ , and  $C_5$ , which altogether represent the feed-forward amplification (gene transcription) mechanism, while the T-invariants (9)–(13) form three other disjunctive T-clusters  $C_6, C_7$ , and  $C_8$ . A subsequent combination of the modules express a specific pathway of the network switch from the steady state ( $C_6$ ) at temperature 37C to the gene transcription ( $C_7$ ) as temperature raises to 42C and then misfolded protein repairing mechanism ( $C_8$ ), finally the module  $C_6$  is returned as stress went away.

Two different cases of reachability graph have been presented, one leads to infinite graph whereas finite graph generated from an initial marking of the Petri net. A deadlock condition has been showed in Proposition 1.

The extended version of the HSR model including

phosphorylation regulation should be studied.

#### REFERENCES

- [1] R.-J. Back, T.-O. Ishdorj, and I. Petre, "A petri-net formalization of heat shock response model," in *Proceedings of the Workshop on Natural Computing and Graph Transformations*, I. Petre and G. Rozenberg, Eds. University of Leicester, 2008.
- [2] H. K. Kampinga, "Thermotolerance in mammalian cells: protein denaturation and aggregation, and stress proteins," *J. Cell Science*, vol. 104, pp. 11–17, 1993.
- [3] A. G. Pockley, "Heat shock proteins as regulators of the immune response," *The Lancet*, vol. 362, no. 9382, pp. 469–476, 2003.
- [4] M. P. Kline and R. I. Morimoto, "Repression of the heat shock factor 1 transcriptional activation domain is modulated by constitutive phosphorylation," *Molecular and Cellular Biology*, vol. 17, no. 4, pp. 2107–2115, 1997.
- [5] D. R. Ciocca and S. K. Calderwood, "Heat shock proteins in cancer: diagnostic, prognostic, predictive, and treatment implications," *Cell Stress and Chaperones*, vol. 10, no. 2, pp. 86–103, 2005.
- [6] K. V. Lukacs, O. E. Pardo, M. Colston, D. M. Geddes, and E. W. Alton, "Heat shock proteins in cancer therapy," in *Cancer Gene Therapy: Past Achievements and Future Challenges*, Habib, Ed. Kluwer, 2000, pp. 363–368.
- [7] P. Workman and E. de Billy, "Putting the heat on cancer," *Nature Medicine*, vol. 13, no. 12, pp. 1415–1417, 2007.
- [8] T. R. Rieger, R. I. Morimoto, and V. Hatzimanikatis, "Mathematical modeling of the eukaryotic heat shock response: Dynamics of the hsp70 promoter," *Biophysical Journal*, vol. 88, no. 3, pp. 1646–58, 2005.
- [9] R. Srivastava, M. Peterson, and W. Bentley, "Stochastic kinetic analysis of the escherichia coli stress circuit using  $\sigma^{32}$ -targeted antisense," *Biotechnology and Bioengineering*, vol. 75, no. 1, pp. 120–129, 2001.
- [10] A. Peper, C. Grimbergent, J. Spaan, J. Souren, and R. van Wijk, "A mathematical model of the hsp70 regulation in the cell," *Int. J. Hyperthermia*, vol. 14, pp. 97–124, 1997.
- [11] O. Lipan, J. Navenot, Z. Wang, L. Huang, and S. Peiper, "Heat shock response in cho mammalian cells is controlled by a nonlinear stochastic process," *PLoS Computational Biology*, vol. 3, no. 10, pp. 1859–1870, 2007.
- [12] I. Petre, A. Mizera, C. L. Hyder, A. Mikhailov, J. E. Eriksson, L. Sistonen, and R.-J. Back, "A new mathematical model for the heat shock response," in *Algorithmic Bioprocesses*, J. Kok, Ed. Springer, 2008.
- [13] I. Petre, C. L. Hyder, A. Mizera, A. Mikhailov, J. E. Eriksson, L. Sistonen, and R.-J. Back, "Two metabolites are enough to drive the eukaryotic heat shock response," *manuscript*, 2008.
- [14] W. Reisig, *Petri Nets: An Introduction*. Springer, 1985.
- [15] —, *A Primer in Petri Net Design*. Springer, 1992.
- [16] E. G. Belau, F. Schreiber, M. Heiner, A. Sackmann, B. Junker, S. Grunwald, A. Speer, K. Winder, and I. Koch, "Modularization of biochemical networks based on classification of petri net t-invariants," *BMC Bioinformatics*, vol. 9, no. 1, 2008. [Online]. Available: <http://dx.doi.org/10.1186/1471-2105-9-90>
- [17] K. Backhaus, B. Erichson, W. Plinke, and R. Weiber, "Multivariate analysis methods: An application-oriented introduction (in german)," vol. 10, 2003.
- [18] P. Rousseeuw, "Silhouettes: a graphical aid to the interpretation and validation of cluster analysis," *Journal of Computational and Applied Mathematics*, vol. 20, 1987.
- [19] (2008) Winidams. [Online]. Available: <http://www.unesco.org/idams>
- [20] (2008) Pina. [Online]. Available: <http://www-dssz.informatik.tu-cottbus.de/>
- [21] (2008) Wilma. [Online]. Available: [Wilmascope. http://wilma.sourceforge.net/](http://wilma.sourceforge.net/)
- [22] K. Voss, M. Heiner, and I. Koch, "Steady state analysis of metabolic pathways using petri nets," *Journal In Silico Biology*, vol. 3, no. 0031, pp. 367–387, 2003.
- [23] M. Heiner and I. Koch, "Petri net based model validation in systems biology," in *ICATPN*, 2004, pp. 216–237.
- [24] I. Koch and M. Heiner, *Petri Nets in Biological Network Analysis*, ser. Wiley & Sons Book Series on Bioinformatics, 2008, ch. Analysis of biological networks, pp. 139–179.